THE ASTROPHYSICAL JOURNAL, 324:749–766, 1988 January 15

A FIVE-BAND STUDY OF SPIRAL GALAXIES: X-RAY, OPTICAL, NEAR- AND FAR-INFRARED, AND RADIO CONTINUUM CORRELATIONS

G. FABBIANO, I. M. GIOIA,[1] AND G. TRINCHIERI[2]
Harvard-Smithsonian Center for Astrophysics
Received 1986 December 5; accepted 1987 June 30

ABSTRACT

We present a statistical analysis of the relationships between radio continuum, far- and near-infrared emission, blue light, and X-ray emission of spiral galaxies. We find differences between early (Sa–Sb) and late-type (Sc–Sm/I) spiral galaxies, both in the strengths of the correlations and in the functional relationships between the variables. In particular, the correlations of the radio continuum and far-infrared luminosities with the other luminosities present more scatter in early-type spirals. These also tend to be overluminous in the blue, *H*, and X-rays for a given radio luminosity when compared with late-type spirals. A similar effect is seen at least for the *H* luminosity when compared with the far-infrared. These effects could be explained with the presence of large bulge components in early-type spirals contributing to the blue, *H*, and X-ray emission, but not to the radio continuum and the far-infrared. The relationships between the variables in late-type spirals suggest a common disk/arm origin for the emission at different wavelengths. Their functional dependences could be consistent with a steeper initial mass function and an obscured compact starburst component in the more luminous galaxies. If the latter dominates the far-infrared emission in these galaxies, the close link between far-infrared and radio emission suggests that the sources of cosmic-ray electrons belong predominantly to the younger Population I component in high-luminosity late-type spirals. However, a link between the radio emission and an older disk component cannot be ruled out in the low-luminosity galaxies. The previously reported link between X-ray and radio emission is also comparatively strong and might imply a physical or evolutionary connection between X-ray and cosmic-ray sources.

Subject headings: galaxies: photometry — galaxies: stellar content — galaxies: X-rays — radio sources: galaxies

I. INTRODUCTION

Correlations between optical and near-infrared emission properties of spiral galaxies have been widely used to gain an understanding of their structure, stellar content, and evolution (e.g., Tully, Mould, and Aaronson 1982; Whitmore 1984). Correlations between the radio continuum emission and optical properties have also been sought to explain the origin of cosmic rays, the properties of magnetic fields, and the effects of density waves (e.g., Hummel 1981; Klein 1982; Kennicutt 1983; Beck and Reich 1985). Surveys of galaxies in two other major bands are now available: in X-rays with the *Einstein Observatory* and in the far-infrared with *IRAS*. The use of these new windows has contributed novel insight into the properties of normal galaxies (e.g., Fabbiano 1986; de Jong 1986), and provides the opportunity to explore galaxy properties using a wide array of different indicators.

The study of single correlations between variables, although offering valuable clues, could also be misleading, since correlations might arise as a consequence of some stronger, more direct link between variables that are not included in the analysis (e.g., Whitmore 1984; Fabbiano and Trinchieri 1985, hereafter FT85). This point is well illustrated by the contradictory conclusions reached by looking separately at the correlations between radio continuum and either X-ray (FT85) or far-infrared emission (Helou, Soifer, and Rowan-Robinson 1985; de Jong *et al.* 1985) in spiral and irregular galaxies. While the former correlation was interpreted as suggesting a link between the radio emission (and thus the cosmic-ray production) and the general, young and older Population I (as originally suggested by van der Kruit, Allen, and Rots 1977; Hummel 1981), the latter was considered as the final demonstration of a very young Population I origin of the radio emission (e.g., Lequeux 1971; Klein 1982; Kennicutt 1983). To address this particular problem, and to gain a general picture of the global emission properties of spiral galaxies, we have carried out a statistical analysis of the emission in the five well-observed wavelength regions: radio continuum (20 cm), far-infrared (60–100 μm), near-infrared (1.65 μm, *H*), optical (*B*), and X-rays (0.2–3.5 keV); we report the results here.

In this paper we look for correlations between these five wave bands; we pay close attention to the relative strength of these multiband correlations and to the slopes of the relationships; and we explore the effect of the Hubble type on these relationships, by studying separately early-type spirals (Sa–Sb) and later systems. The samples used in this analysis are described in § II; the methods followed and our results in comparison with previous work are given in § III. In § IV we discuss their implications. Our conclusions are summarized in § V.

Throughout this paper we will adopt $H_0 = 50$ km s^{-1} Mpc^{-1}.

II. THE SAMPLES

Two samples of spiral galaxies were used in this analysis. They are largely nonoverlapping and were selected and observed for different reasons. The first (the VLA sample) is a statistically complete sample of spiral galaxies of selected early and late morphological types, which was observed with the

[1] On leave of absence from Istituto di Radioastronomia del CNR, Bologna, Italy.
[2] Presently at Osservatorio Astrofisico di Arcetri, Firenze, Italy.

TABLE 1

THE VLA SAMPLE

Galaxy NGC (1)	T (2)	D (Mpc) (3)	log ℓ_B (erg $s^{-1}Hz^{-1}$) (4)	log ℓ_R (erg $s^{-1}Hz^{-1}$) (5)[a]	log L_{FIR} (erg s^{-1}) (6)
278	3	18.6	28.93	28.70	43.74
672	6	12.9	28.67	27.38	42.63
891	3	15.6	29.39	29.28	44.10
				(29.35)	
925	7	15.8	29.16	28.08	43.07
				(28.29)	
949	3	17.1	28.45	27.82	42.90
2683	3	8.0	28.80	27.74	42.56
2841	3	14.3	29.34	28.22	42.79
				(28.37)	
3184	6	12.1	28.84	27.90	42.68
				(28.17)	
3190	1	27.7	29.20	28.59	43.34
3319	6	15.5	28.59	26.94	42.20
3432	9	12.1	28.53	28.16	42.72
3504	2	29.6	29.17	29.51	44.03
3556	6	15.8	29.14	28.90	43.67
3583	3	43.7	29.39	29.08	44.01
3675	3	15.8	29.08	28.18	43.32
3690	9	61.9	29.64	30.48	45.35
3718	1	21.6	29.22	28.18	<42.55
3769	3	15.8	28.39	27.52	42.72
3898	2	25.2	29.14	27.73	<42.55
3982	3	23.9	28.85	28.63	43.46
4102	3	19.0	28.65	29.04	44.02
4157	3	17.0	28.90	28.80	43.49
4244	6	5.0	28.24	<25.91	<41.20
4242	8	11.3	28.37	27.09	-----
4274	2	17.6	29.08	27.42	43.07
4314	1	17.0	28.65	27.62	42.87
4395	9	6.1	28.16	27.34	41.80
4448	2	13.1	28.54	26.62	42.36
4490	7	12.0	29.01	29.09	43.60
4559	6	15.4	29.19	28.28	43.06
				(28.71)	
4565	3	23.4	29.84	28.87	43.53
4618	9	11.3	28.49	27.66	42.59
4631	7	12.1	29.31	29.17	43.75
				(29.35)	
4656	9	12.5	28.74	28.02	42.44
				(28.35)	
4725	2	23.3	29.71	28.39	<42.87
4736	2	6.9	29.06	28.12	43.26
				(28.19)	
4800	3	16.2	28.46	27.82	43.03
4826	2	7.0	28.97	27.78	43.10
5204	9	6.6	27.85	26.76	41.87
5457	6	7.4	29.31	28.16	42.86
				(28.75)	
5474	6	7.9	28.12	26.48	41.86
5585	7	8.8	28.24	26.81	41.84
5985	3	53.9	29.78	28.50	43.57
6946	6	6.7	28.84	28.79	43.25
				(28.91)	
7217	2	24.7	29.40	28.10	43.46
7741	6	20.6	28.81	27.49	42.90

[a] The numbers in parentheses are from Hummel 1980.

VLA to investigate specifically the morphological dependence of the correlation between radio continuum and optical emission (Gioia and Fabbiano 1987). The second (the X-ray sample) is the sample observed in X-rays with the *Einstein Observatory*. This sample, although not statistically complete, is representative of normal spiral and irregular galaxies (FT85). Radio continuum, optical, and far-infrared measurements are available for the VLA sample; all of these, and also near-infrared and X-ray measurements, are available for the X-ray sample. The use of both samples allows us to check for possible selection biases that might affect the results of the X-ray sample. Also, it gives us twice as many galaxies with which to study the relationships between R, FIR, and *B*, thus allowing us to constrain them more effectively.

a) The VLA Sample

This is a statistically complete magnitude-limited sample of 46 spiral galaxies (see description in Gioia and Fabbiano 1987). Of these, 25 have morphological parameters $T = 1$–3 (T is from de Vaucouleurs, de Vaucouleurs, and Corwin 1976, i.e., Sa–Sb), and 21 have $T = 6$–9 (Scd–Sm). All but one were detected in radio continuum at 20 cm with the VLA. The data are published in Gioia and Fabbiano (1987), but no statistical analysis was done in that paper.

Table 1 lists the galaxies in this sample, together with their morphological parameter T, their distance in megaparsecs estimated from the *Revised Shapley-Ames Catalog of Bright Galaxies* (Sandage and Tammann 1981), their monochromatic optical (B) luminosity l_B, their monochromatic radio continuum (20 cm) luminosity l_R, and their "total" far-IR luminosity $L_{\rm FIR}$. The radio and optical luminosities were derived from the 20 cm VLA flux densities and optical magnitudes listed in Table 1 of Gioia and Fabbiano (1987). In the case of NGC 3504, which was not detected because of interference in the VLA data, we use the previously published 20 cm flux density of Hummel (1980). For some of the galaxies the VLA flux densities are smaller than previously reported measurements (see Gioia and Fabbiano 1987). For these galaxies the 20 cm luminosities derived from Hummel (1980) are given in parentheses in Table 1. We will consider the effect of this discrepancy in our statistical analysis. The far-infrared luminosity $L_{\rm FIR}$ was derived from the *IRAS* band fluxes (FIR) listed in *Cataloged Galaxies and Quasars Observed in the IRAS Survey* (1985). In cases where more than one source was detected within a galaxy, the sum of all the fluxes was used.

b) The X-Ray Sample

The second sample is composed of 51 galaxies observed in X-rays with the *Einstein Observatory*. Forty-eight of these were in the sample studied by FT85. To these we have added NGC 5194 (M51; Palumbo *et al.* 1985), NGC 4631, and NGC 6946. The latter two, although originally observed in X-rays as part of a survey of peculiar galaxies, are similar to normal spirals in their X-ray properties (Fabbiano, Feigelson, and Zamorani 1982). The statistical analysis of this sample was performed originally by FT85. The present analysis includes the far-infrared luminosities, which were not available to FT85, and also applies newer techniques, which allow a more complete analysis (see § III and the Appendix).

Table 2 lists the 51 galaxies in the X-ray sample, together with the morphological type, the assumed distances, and monochromatic continuum luminosities at 20 cm (l_R), 1.65 μm (l_H), B (l_B), and X-rays (l_x), as described in FT85. It also lists their far-infrared luminosities $L_{\rm FIR}$. These were derived in the same way as those of the VLA sample, with the exception of M31 and M33. Since the far-infrared flux density of these two nearby galaxies is seriously underestimated in the *IRAS* catalog, we used instead flux densities estimated from pointed *IRAS* data (as quoted by Helou, Soifer, and Rowan-Robinson 1985).

The galaxies in the X-ray sample have morphological types ranging from S0/a to Im ($T = 0$–10). For the purpose of this paper we have grouped together early-type spirals with $T = 0$–3 (S0/a–Sb), and late-type spirals with $T = 4$–10 (Sbc–Im). The two subsamples consist of 22 and 29 (only four of which are borderline $T = 4$) galaxies, respectively. Six galaxies (NGC 2841, NGC 4244, NGC 4631, NGC 4826, NGC 5457, and NGC 6946) are common to both the VLA and the X-ray samples. The distances and l_B for some of these galaxies are slightly different in Tables 1 and 2 because different sources for these quantities were used in the two samples (Gioia and Fabbiano 1987 and FT85, respectively). The different values are, however, within the scatter of the correlations, and these differences do not affect the results of the analysis.

III. DATA ANALYSIS

a) Results

Figures 1 and 2 show the scatter diagrams of all the variables considered in the VLA and X-ray samples. These figures show immediately that (1) clear correlations between all the variables exist in late-type spirals, while a larger scatter and in some cases no correlations are visible in early-type spirals; (2) correlations between different variables may differ in the relative amount of scatter and in the slopes suggested by the distributions of the points in the diagrams;[3] (3) these correlations are not the result of a segregation of galaxies of given morphological types into different limited ranges of luminosity, since they are present within each morphological type.

These visual impressions are confirmed and quantified by our statistical analysis (see Appendix). In the early-type spirals we find that the most significant correlations by far are (R, FIR), (H, B), and (X, B), and that the other correlations present a significant amount of scatter. In the late-type spirals, instead, all the correlations are very strong. In particular, the correlations (R, FIR), (R, X), and (H, B) all have a probability of arising by chance of $P \ll 5 \times 10^{-7}$; those between (B, X), (X, FIR), and (B, FIR) all have $P \ll 5 \times 10^{-5}$. We also find that different correlations may follow different power-law relationships. Since most of these relationships are ill defined in the early-type spirals, we only show the average best-fit lines for the late-type sample in Figure 2. These lines are also plotted on the scatter diagrams of the early-type sample in the same figure, for ease of comparison. Of the most significant correlations, only (X, B) and (R, FIR) are consistent with a power-law exponent $\alpha \approx 1$. Although less well defined, (FIR, H) and (R, H) could also have $\alpha \approx 1$. The other correlations are described by power-law exponents definitely different from unity: in particular, the regression lines for the (B, H), (B, R), (X, R), (B, FIR), and (X, FIR) correlations all have power-law exponents in the range of $\alpha \approx 0.5$–0.7; the regression lines for the inverse

[3] In the following, when we refer to a correlation with the notation (Y, X) in the parametric analysis, we imply that Y is the dependent and X is the independent variable. When we refer to a correlation as "steep" or "flat," it is with reference to this notation.

TABLE 2

THE X-RAY SAMPLE

Galaxy NGC (1)	T (2)	D (Mpc) (3)	log ℓ_R (erg s^{-1}Hz^{-1}) (4)	log ℓ_H (erg s^{-1}Hz^{-1}) (5)	log ℓ_B (erg s^{-1}Hz^{-1}) (6)	log ℓ_x (erg s^{-1}Hz^{-1}) (7)	log L_{FIR} (erg s^{-1}) (8)
224	3	0.7	27.66	29.40	28.97	21.66	42.60
247	7	3.4	26.49	28.08	28.25	21.30	<41.15
253	5	3.4	28.88	29.26	28.83	21.78	43.72
520	0	46.7	29.66	29.76	29.47	22.90	44.63
598	6	0.7	27.28	28.05	28.12	21.01	42.27
628	5	3.4	27.45	28.00	28.00	20.79	41.53
1073	5	26.4	<28.62	-----	29.08	22.32	43.27
1097	3	24.5	29.65	-----	29.54	23.18	44.27
1300	4	30.4	28.58	29.58	29.42	<22.65	43.38
1313	7	4.8	28.06	-----	28.52	21.71	42.31
1350	2	29.3	<28.11	-----	29.27	<22.63	<42.84
1398	2	30.4	28.22	30.15	29.59	22.59	43.15
1559	6	20.5	29.36	29.04	29.20	22.66	43.87
LMC	9	0.05	-----	-----	28.15	20.59	-----
2366	10	3.2	-----	26.78	27.48	<20.60	41.30
2403	6	3.2	27.58	28.52	28.43	21.47	42.23
2613	3	28.9	28.86	29.94	29.56	<22.80	43.67
2763	6	10.7	27.81	-----	27.88	21.48	42.29
2775	2	19.3	<28.36	29.52	28.96	22.24	42.92
2835	5	10.7	27.89	28.56	28.41	<21.82	42.56
2841	3	12.0	28.22	29.49	29.06	22.08	42.64
2848	5	10.7	-----	-----	27.73	<21.42	42.14
2903	4	7.6	28.45	29.25	28.87	22.07	43.19
3031	2	3.2	27.68	29.36	28.85	22.35	42.23
3077	0	3.2	<26.80	27.65	27.64	20.37	41.99
3368	2	16.0	28.44	29.75	29.22	21.95	43.29
3593	0	16.0	28.45	-----	28.64	22.03	43.52
3628	3	16.0	29.19	29.71	29.35	22.89	43.95
4236	8	3.2	<26.80	27.48	28.02	20.91	41.35
4244	6	5.0	<27.18	27.99	28.24	21.14	<41.20
4449	10	5.0	27.82	28.04	28.32	21.50	-----
4579	3	21.7	29.08	29.75	29.27	22.49	43.32
4594	1	19.3	28.92	30.39	29.80	23.04	43.05
4631	7	12.1	29.35	-----	29.31	22.29	43.75
4643	0	25.4	<28.59	29.71	29.04	<22.87	42.49
4753	0	22.7	<28.49	29.82	29.27	22.30	43.06
4826	2	5.0	27.43	29.05	28.54	21.56	42.81
5068	6	7.9	27.85	-----	28.31	21.58	42.35
5078	1	7.9	-----	-----	27.72	21.22	42.72
5101	0	7.9	<27.57	-----	27.90	<21.63	41.75
5194	4	11.0	29.22	-----	29.25	22.53	43.56
5236	5	7.9	29.10	29.53	29.39	22.46	43.67
5253	0	7.9	27.62	27.91	28.38	21.03	43.02
5457	6	7.2	28.72	29.37	29.25	22.24	42.90
5566	2	34.6	<28.86	-----	29.51	<22.80	43.18
5907	5	18.4	28.67	29.59	29.22	22.24	-----
6744	4	10.4	28.57	29.18	29.44	22.30	42.56
6946	6	6.7	28.91	-----	28.84	22.59	43.25
7793	8	3.4	26.80	28.00	28.04	21.30	41.92
IC342	6	4.6	28.85	----	28.91	21.88	43.12
IC2574	9	3.7	<27.04	27.18	27.67	20.77	41.05

relationships are less well defined, but nonetheless all have exponents $\alpha \sim 1.3$.

Since the behavior of the relationships between R, FIR, and *B* is similar in the statistically complete VLA sample and in the X-ray sample, we resolved to add the two samples together to increase the significance of our regression analysis for these three variables. The resulting sample and the results of the analysis are shown in Figure 3 and in the Appendix. By examining this figure (and also Fig. 2), we notice that the points in some of the early-type sample diagrams are displaced on one side of the average line of the corresponding late-type relationships. In particular, in early-type spirals we find a relative deficiency of radio emission (R) with respect to FIR, *H*, *B*, and X, and a relative deficiency of far-infrared (FIR) with respect to *H*. Two of these effects (the R–*B* and the R–X) have been previously discussed (Hummel 1981; FT85). The R–FIR effect could be due to a bias resulting from the *IRAS* beam size, which would not allow the detection of the entire FIR emission of the more extended galaxies (see § III*b*), since the late-type subsample is dominated by galaxies with large angular diameters. We checked this possibility by comparing galaxies with small ($D_{25} < 5'$) and large ($D_{25} \geq 5'$) isophotal diameters, and

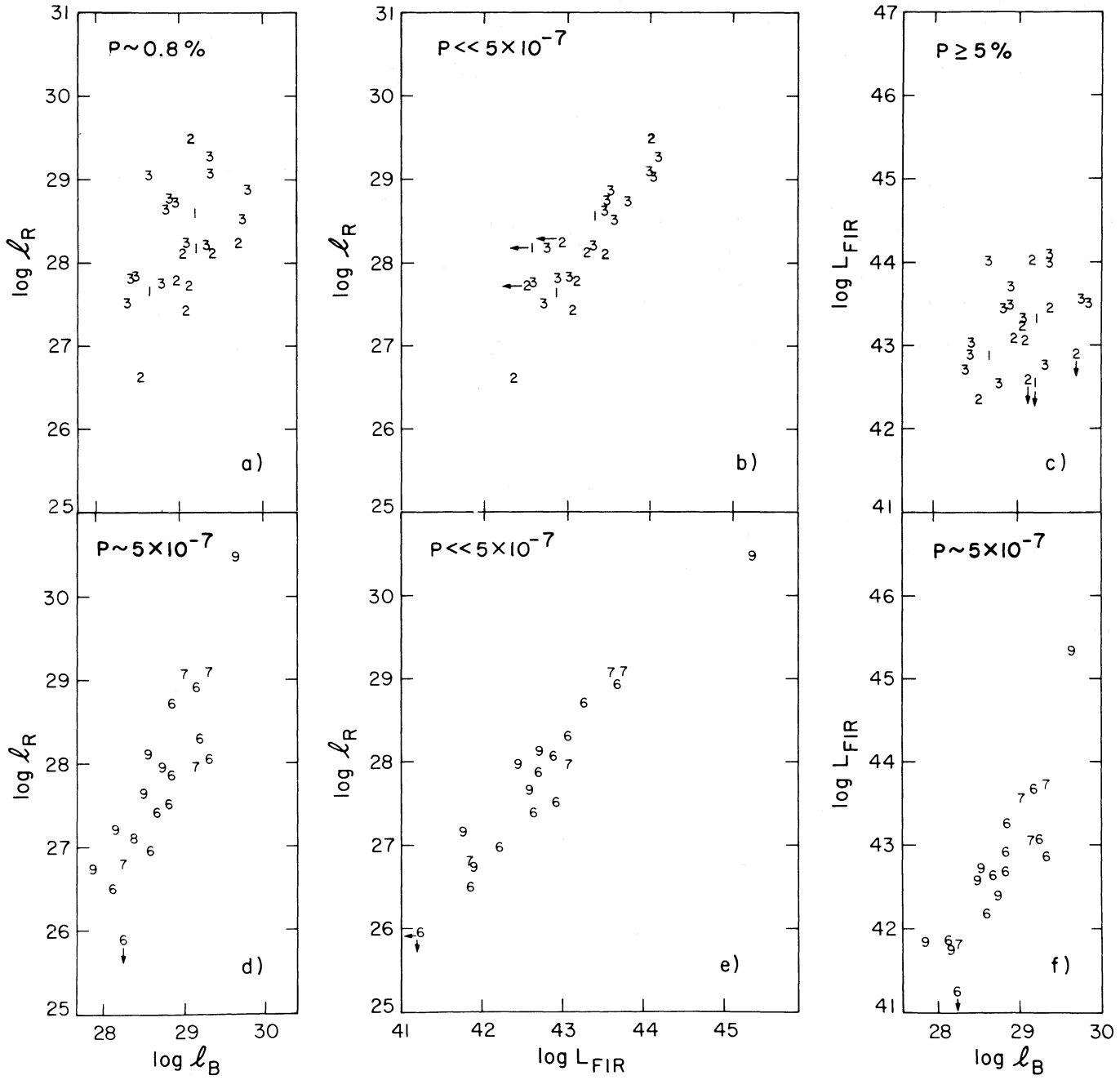

FIG. 1.—Scatter diagrams of log l_R, log l_B, and log L_{FIR} for the early-type (*a*, *b*, *c*) and late-type (*d*, *e*, *f*) spiral galaxies of the VLA sample. The numbers in the plots indicate the morphological parameter T of each galaxy. The monochromatic luminosities l_B and l_R are in units of ergs s^{-1} Hz^{-1}. The far-infrared luminosity L_{FIR} is in units of ergs s^{-1}. The nonparametric Spearman rank probabilities of chance correlation (see Appendix) are indicated in each case.

we found indeed a zero-point shift in R–FIR in the expected sense.

Making use of the extended sample of Figure 3, we can also examine in a quantitative way the possibility that the correlations found between luminosities might be a consequence of the well-known correlation between morphological type and luminosity. Figure 4*a* shows the (R, FIR) correlation for galaxies with morphological parameters $T = 3$ and $T = 6$. We have chosen these morphological types because they are best represented in our sample. The figure shows that while the distribution of galaxies with $T = 3$ is displaced toward higher luminosities, as expected because of the well-known type-luminosity effect, very significant correlations are independently present in the two groups of galaxies. A second example is given in Figure 4*b*, which shows the (FIR, *B*) correlation for late-type spirals. Again, all morphological types follow the general trend.

We then addressed the question of which correlations are likely to be fundamental and which ones are instead the result of other, stronger links. The results of the Spearman partial rank test (see Appendix) for the X-ray sample are shown in Figures 5 and 6. By testing all possible combinations of three

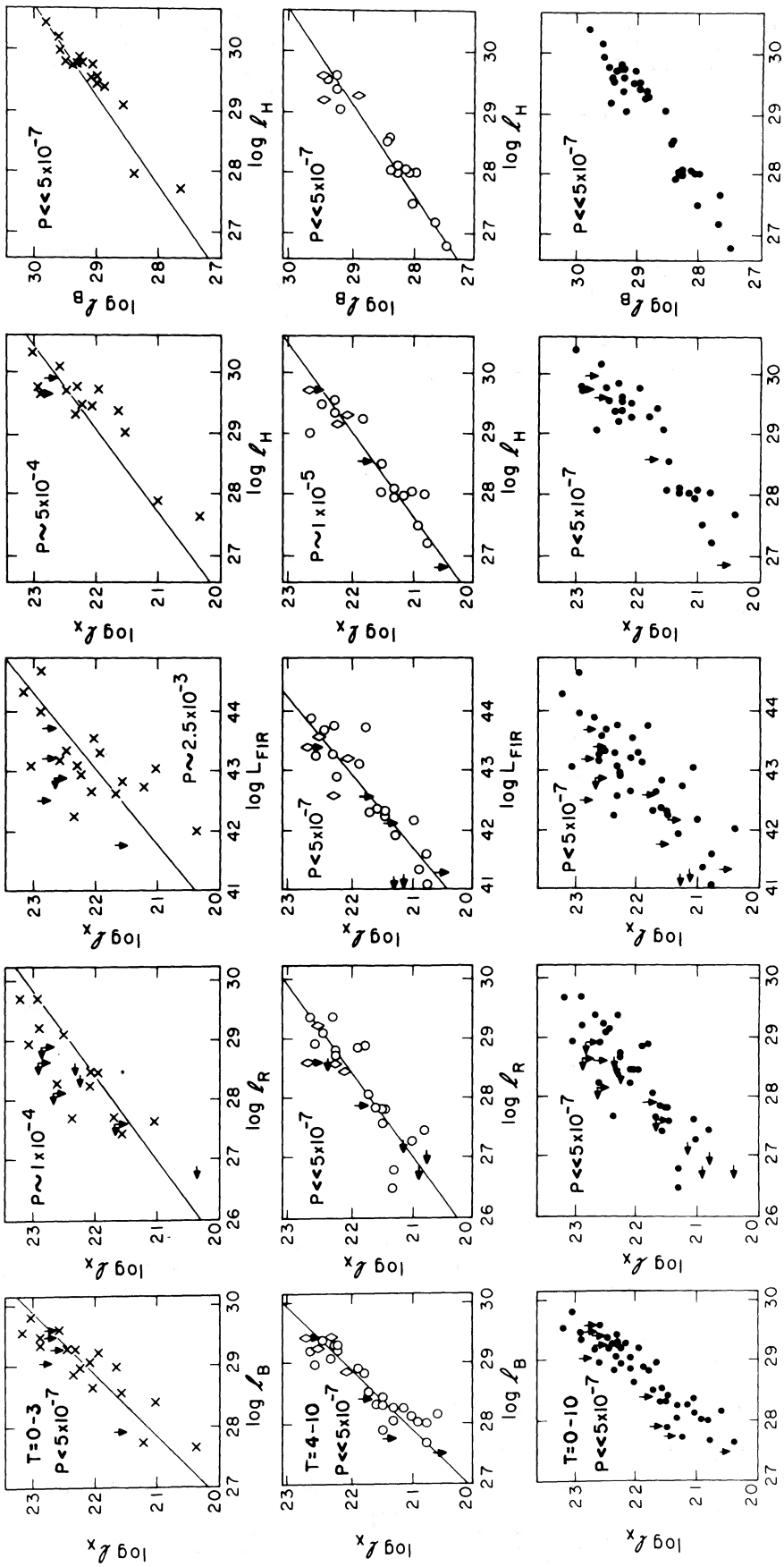

FIG. 2.—Scatter diagrams of log L_x, log l_B, log l_R, log l_H, and log L_{FIR} for the X-ray sample of spiral galaxies. Crosses identify the early-type spirals (T = 0–3), open circles the late-type galaxies (T = 5–10), diamonds the four galaxies with T = 4, and dots the entire range of morphological types (T = 0–10). The nonparametric Spearman rank probabilities of chance correlation (see Appendix) are indicated in each case. The diagonal lines represent the "average" functional relationships derived for the late-type spirals.

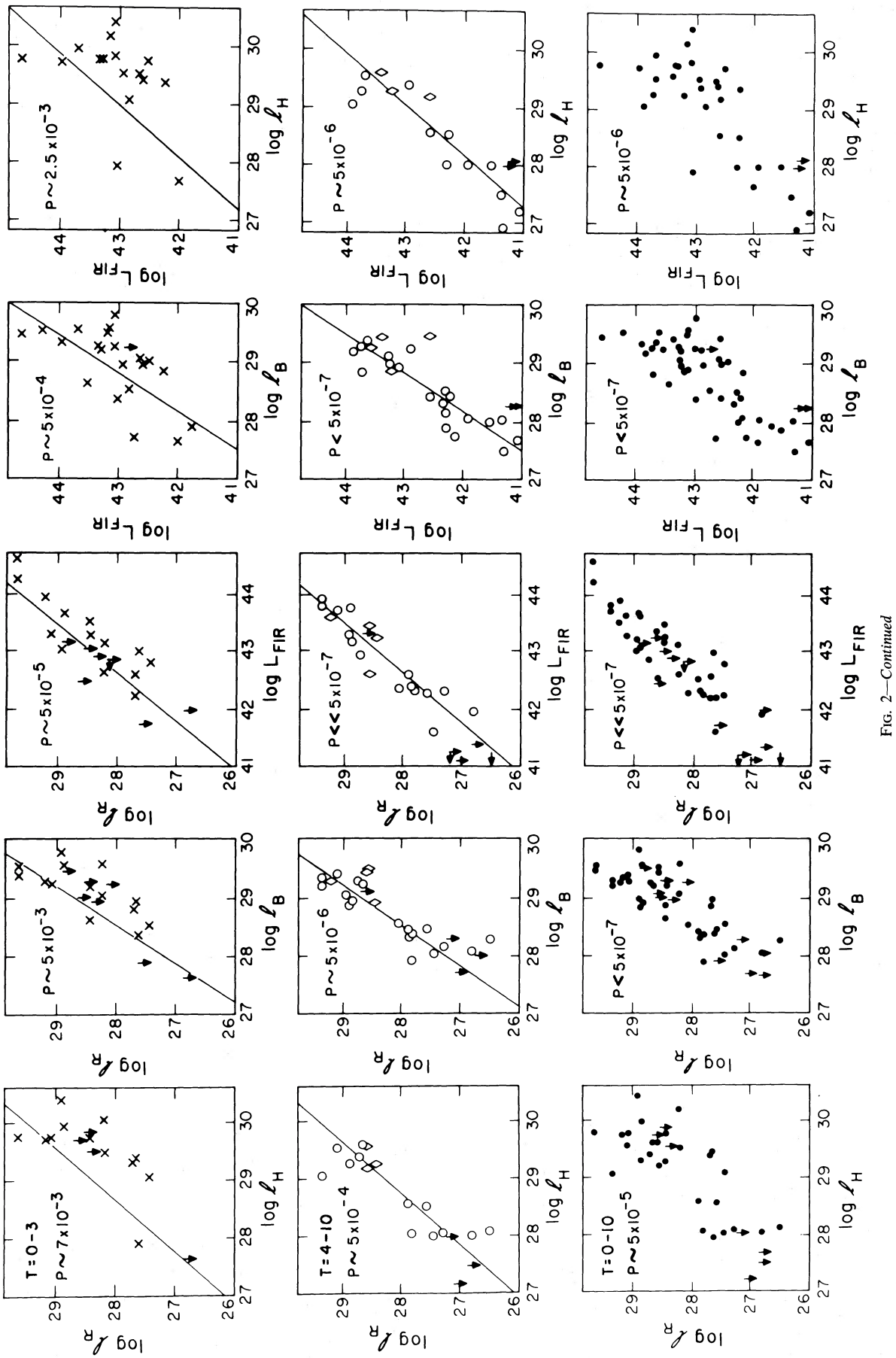

FIG. 2—*Continued*

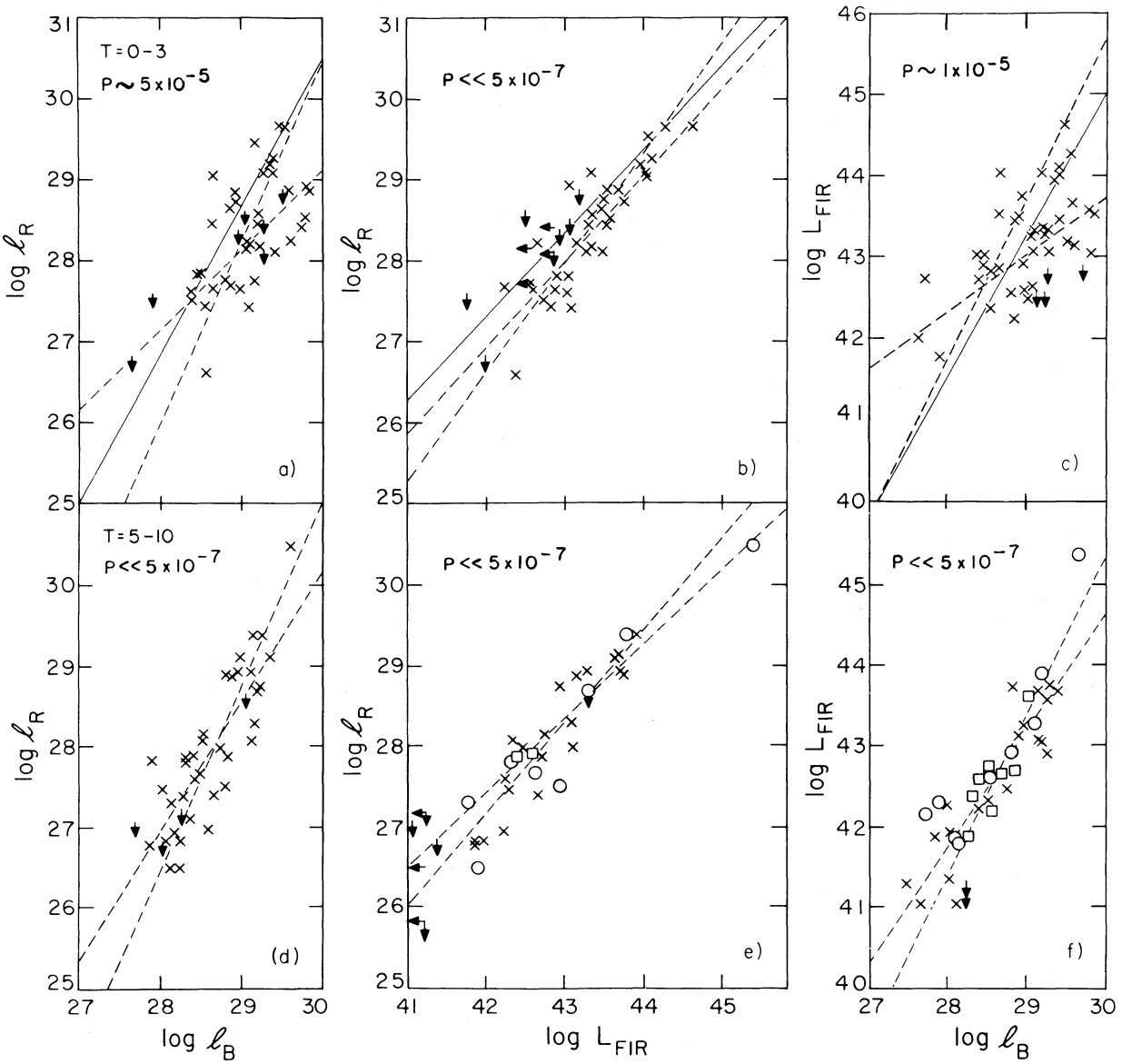

FIG. 3.—Scatter diagrams of log l_R, log l_B, and log L_{FIR} for the "joint" sample. The nonparametric Spearman rank probabilities of chance correlation (see Appendix) are indicated in each case. The dashed lines are the best-fit regression lines. The thin solid lines in (*a*)–(*c*) represent the average regression lines for the corresponding late-type (T = 5–10) correlations. In (*e*) and (*f*) galaxies with photometric diameters $D_{25} \leq 5'$, $5' < D_{25} \leq 7'$, and $D_{25} > 7'$ are represented with circles, squares, and crosses, respectively.

and four variables, we find that in the early-type spirals the primary correlations are those between near-infrared and blue (*H*, *B*) and radio and far-infrared (R, FIR), followed by those between blue and X-rays (*B*, X) and X-rays and radio (X, R). In the late-type spirals the primary correlations are (*B*, X) and (R, FIR), followed by (*H*, *B*) and (X, R). Concentrating on the late-type sample, we find that the correlations between X and both *B* and FIR are equally strong; X is better correlated with R than with *B*; R is better correlated with FIR than with X; and there are no links between R and both *H* and *B*. These results can be summarized by arranging the five variables in a "correlation chain" as *H*–*B*–X–R–FIR, in which a given variable is primarily linked with the two adjacent variables.

b) Potential Biases

We have considered the effect of biases in our samples. Possible sources are distance effects (i.e., Malmquist effect and the uncertainties in the distances), beam-size effects, and the handling of limits.

i) *Malmquist Effect*

This bias is unlikely to be responsible for the correlations because, except for an optical selection, there was no other *a priori* flux selection in either sample, and the upper limits all follow the trend suggested by the detections. These limits were used in the parametric analysis, thus avoiding the danger of introducing *a posteriori* flux selections. Given our sample selec-

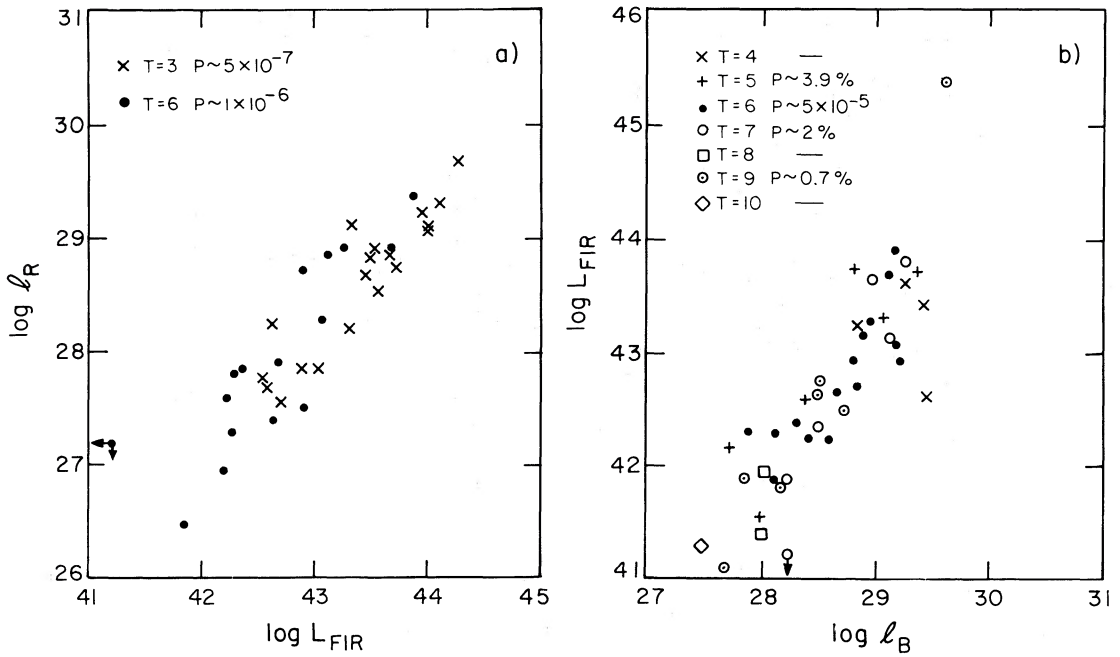

FIG. 4.—(*a*) The (R, FIR) correlations for galaxies of different morphological types ($T = 3$ and $T = 6$); (*b*) the (FIR, *B*) correlations for galaxies of different "late" ($T \geq 4$) morphological types. The probabilities given in the figure are nonparametric Spearman rank probabilities of chance correlation.

tion, correlations between luminosities may well be less affected by a distance bias than correlations between fluxes, where a "true" correlation may be washed out by a distance effect (see Fabbiano, Feigelson, and Zamorani 1982 and Appendix A in Feigelson and Berg 1983). In any case, we analyzed the relationships between fluxes and found that similar correlations are also present, although with less significance (see also FT85). Moreover, the nonlinear slopes observed in many instances cannot be caused by a Malmquist bias, which would only stretch the points along a 45° line (slope = 1) in the correlation plots.

ii) *Beam-Size Effects*

A beam-size effect in principle could be responsible for turning an intrinsic linear correlation into a nonlinear one. This would happen if one of the two variables under examination has been observed with a small beam size and if the sample selection is such that more luminous galaxies are sys-

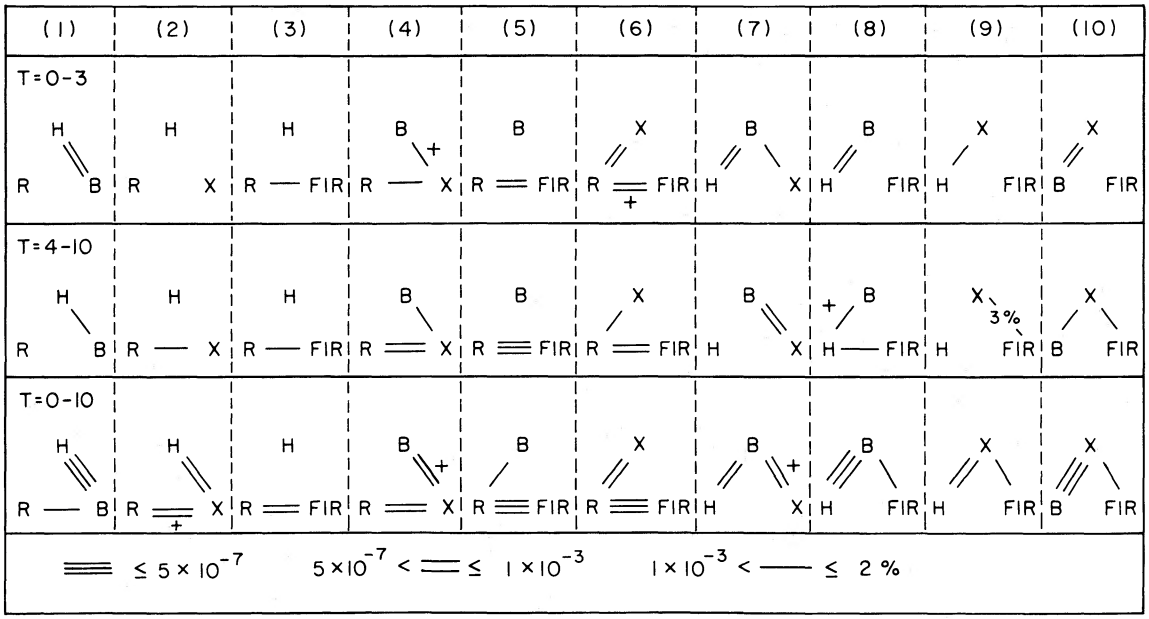

FIG. 5.—Plots of the results of the Spearman partial rank tests for the X-ray sample on groups of three variables. Stronger correlations are represented with a larger number of lines between the variables.

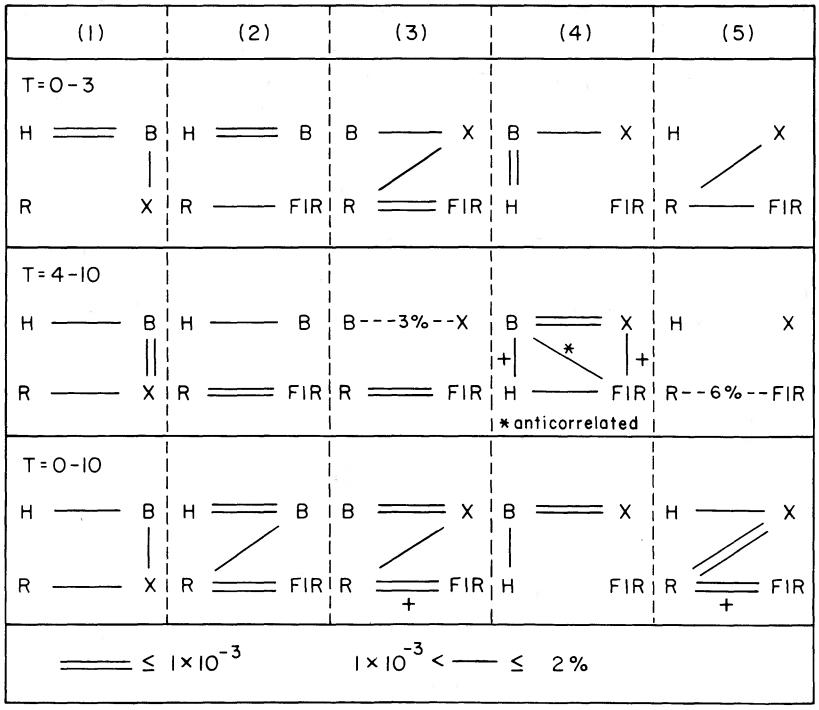

FIG. 6.—Plots of the results of the Spearman partial rank tests for the X-ray sample on groups of four variables. Stronger correlations are represented with a larger number of lines between the variables.

tematically farther away and therefore smaller in angular diameter. Correlations with power-law exponents steeper than unity are observed, e.g., in the late-type samples, (R, *B*), (*H*, *B*), (FIR, *B*), and (FIR, X). The *B* and *H* integral luminosities used should not suffer from a beam-size effect (see FT85). The X-ray luminosities were derived from areas comparable to that used to derive *B* (see Long and Van Speybroeck 1983; FT85), and detailed comparison in a number of galaxies shows that the X-ray emission is coextensive with the optical emission (see Fabbiano 1986; Fabbiano and Trinchieri 1987). They could be underestimated only perhaps in the resolved nearby galaxies (e.g., LMC, M31, M33) where diffuse low surface brightness emission would be hard to distinguish from the instrumental field background. The proportionality found between *B* and X supports our conclusion that beam-size effects between these two quantities are not a major concern.

About 60% of the galaxies of the VLA sample and most of the galaxies of the X-ray sample have isophotal diameters $D_{25} \geq 5'$. Their far-infrared flux therefore could be underestimated because of the *IRAS* beam size. Detailed mapping of spiral galaxies in fact shows that the far-infrared and optical emissions are generally coextensive (Rice *et al.* 1987). However, it is unlikely that this could introduce the steep correlations, for the following reasons: (1) there is no luminosity-distance correlation in either the VLA or X-ray subsample of late-type galaxies, if we exclude NGC 3690 in the VLA sample and four high-luminosity galaxies ($l_B > 10^{29}$) in the X-ray sample (Fig. 7). The exclusion of these galaxies from the correlations does not change the observed trends and does not affect the results of our analysis. (2) There is no luminosity–angular diameter dependence. Both small- and large-diameter galaxies are spread throughout the luminosity range, and they all follow the same correlations (e.g., Figs. 3*e* and 3*f*). (3) A steep correlation between FIR and *B* was also found by Gavazzi, Cocito, and Vettolani (1986) using a substantially different sample, dominated by small-diameter galaxies. (4) We have confirmed this result independently, by reanalyzing the sample of small-size spirals of Rowan-Robinson and Crawford (1986) (§ IV*b*[iii]).

Similar remarks apply to the correlations with the radio power. The steep correlation between radio and *B* luminosities, in particular, was originally found by Fabbiano, Trinchieri, and Macdonald (1984) in the Gioia and Gregorini (1980) sample, observed at 408 MHz with a wide (2.5 × 4.5) beam. The linearity ($\alpha \approx 1$) of the (R, FIR) correlation, observed in our sample and in work by other authors (Helou, Soifer, and

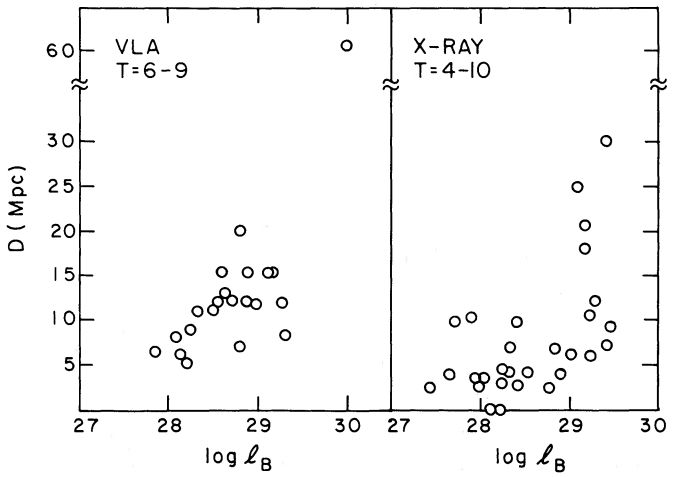

FIG. 7.—Plots of distance in megaparsecs vs. the logarithm of l_B for late sample galaxies: (*left*) the VLA sample; (*right*) the X-ray sample. Distance and luminosity are largely uncorrelated in these samples.

Rowan-Robinson 1985; de Jong *et al.* 1985; Gavazzi, Cocito, and Vettolani 1986), also argues against strong beam-size systematics, unless they affect both R and FIR by similar amounts. As mentioned in § II*a*, the radio flux densities of the more extended galaxies tend to be underestimated by the VLA survey of Gioia and Fabbiano (1987). The use of different measurements for these galaxies does not, however, change our results (Appendix).

A beam-size effect can be responsible for introducing some scatter in the correlations, since the galaxies in the sample exhibit a well–spread-out range of angular diameters. It cannot, however, be responsible for the larger scatter observed in some of the correlations in early-type spirals, since the same techniques were used for obtaining fluxes in the entire range of morphological types, and the early-type spirals in our samples have on average smaller angular sizes. A beam-size effect could also result in a systematic shift of the zero point of the correlations of the more extended late-type spirals toward smaller values of far-infrared luminosities. This effect may be observed in the (R, FIR) correlation (§ III*a*).

iii) *The Upper Limits*

Although the upper limits are included in the parametric analysis, they cannot be included in the nonparametric tests used to compare the relative strength of the correlations. In most instances the number of limits is relatively small and their distribution typically agrees with the distribution of the detections, so that their exclusion should not introduce unwanted biases. In particular, in the VLA sample we have only one radio limit and four far-infrared limits. In the correlations involving X-rays, the effect of the limits was explored in a worst-case scenario by FT85 and was found not to affect the results significantly. In the multivariate analysis the necessity of considering subsamples detected in all the variables leads in certain cases to relatively small working samples. However, the results obtained for different selections of variables (which include different selections of objects) typically are internally consistent (see Appendix and Figs. 5 and 6).

iv) *"Nonintrinsic" Scatter and the Multivariate Analysis*

Caution should be exercised when interpreting the results of the multivariate analysis and comparing good correlations of similar weight, since the spread introduced by measurement errors (e.g., beam-size effects) could be significant. Also, scatter might be introduced by the uncertainties in the distances, which might cause an intrinsically strong nonlinear correlation (power-law exponent not equal to 1) to appear spuriously less strong than a linear one (power-law exponent equal to 1). This could happen because the uncertainties in the distance of individual galaxies will cause the points to move various amounts along 45° lines of differing normalization in the correlation plane, thus worsening intrinsically strong nonlinear correlations. Linear correlations will be less affected, since the points will move along the correlation axis. This effect might be relevant, in particular, when comparing the correlation between R, FIR, and *B* in late-type spirals, since the scatter in the nonlinear (R, *B*) and (FIR, *B*) correlation could be enhanced by uncertainties in the distances. The same applies to the comparison of the (R, X) and (R, FIR) correlations in late-type spirals.

c) Comparison with Other Work

The relationship between radio continuum and blue luminosities of spiral galaxies and their dependence on morphological type were investigated by Fabbiano, Trinchieri, and Macdonald (1984) using the complete sample of Gioia and Gregorini (1980), which, however, contained a large number of upper limits. They reported that R and *B* were very weakly correlated in the early-type spirals, while a steep power law ($l_R \propto l_B^{1.6\pm0.25}$) was found in late-type spirals. Our present results (Table 6 in the Appendix; Figs. 1 and 2) confirm and strengthen those earlier reports.

The presence of a strong linear correlation between radio continuum and far-infrared emission was first reported by de Jong *et al.* (1985) and Helou, Soifer, and Rowan-Robinson (1985) for morphologically heterogeneous samples. More recently, Hummel (1986) and Gavazzi, Cocito, and Vettolani (1986) have reported investigations on the relative strengths of the correlations between R, FIR, and *B*; the latter authors have also investigated their dependence on morphological type. Our sample selection does not allow a direct comparison with Hummel's work, which examined exclusively Sbc galaxies. However, in the joint sample of late-type galaxies our results on the relative strength of the correlations agree with Hummel's. Our results on the functional relationships between radio and *B* emission are in overall agreement with those of Gavazzi, Cocito, and Vettolani (1986). These authors, however, given the large amount of nondetection in their sample, sought relationships between the average values of the variables in luminosity bins, instead of using direct regressional techniques.

Our present results (Appendix, Table 5) are entirely consistent within statistical limits with those of FT85. However, FT85 calculated two-way regressions only for the (X, R) correlation. The extension of this technique to all the correlations in our present work shows that FT85's conclusion of a power-law exponent smaller than unity in the early sample (X, *H*) correlation is probably not correct. Similarly, the conclusion of an exponent of unity for the (X, *B*) correlation in early-type spirals is not as strong as suggested in FT85. Our present conclusions for the correlation between X-ray luminosity and *H*, *B*, and R in late-type spirals are in agreement with those of FT85, and make them stronger, given our more complete correlation analysis.

IV. DISCUSSION

a) Morphological Differences: Disk and Bulge Contributions

While late-type spirals are dominated by the disk/arm stellar component, prominent bulges are present in early-type spirals and account for between ~80% and ~30% of their total optical (*B*) emission (Simien and de Vaucouleurs 1983; Kent 1985). If these bulges also contribute substantially to the near-infrared (*H*) and X-ray bands, but not to the radio and far-infrared emission, then the less well defined correlations and zero-point shifts of the early spiral sample relative to the late spirals (§ III*a*) could be explained. Since the bulge contribution to the emission of early-type spirals is not likely to be correlated with disk properties, one would expect a larger scatter in the correlations for these galaxies, as observed. One would also expect a lack of radio and far-infrared emission in early-type spirals (if these are mainly disk-related properties), relative to the other wavelengths at which bulge emission might give a substantial contribution (i.e., *B*, *H*, X; FT85). As discussed above, there is evidence of this effect. In particular, FT85 showed that the lack of radio continuum relative to the X-ray emission in early spiral galaxies (when compared with later morphological types) can be explained with the presence of a

bulge component in the X-ray emission which is absent in the radio.

Other effects, besides a prominent bulge component in early-type spirals, could also be present and account for some of our results. For example, Hummel (1981) suggested that early-type spirals have intrinsically weaker magnetic fields or a smaller cosmic-ray density in their disks, thus explaining their relative lack of radio emission. However, in his analysis he did not separate the bulge and disk contributions to the optical emission. Any such effect needs to be checked with a study of the detailed surface brightness of a sample of spiral galaxies which would allow for bulge and disk decomposition in different energy bands.

b) *The Nonlinear Relationships in Late-Type Spirals: B, H, and FIR*

Since the statistical properties of early-type spirals are likely to be the result of two equally important components (bulge and disk), which cannot be separated with the present data, we will only consider late-type spirals where the disk dominates (Kent 1985) for the rest of this discussion and investigate what are the implications of our results for the emission properties of disk galaxies. The correlations in these galaxies show little scatter. It is therefore meaningful to consider the functional dependences between the variables, together with the relative strength of the correlations, to get a complete picture of their global emission properties.

As discussed earlier in this paper we find two strong linear correlations, the one between optical (B) and X-ray luminosities, and the one between radio continuum and far-infrared luminosities. The first suggests that X-ray sources are a constant fraction of the blue-emitting stellar population (see FT85); the second suggests that the sources of cosmic rays in spiral galaxies are a constant fraction of the far-infrared emitting population (e.g., de Jong *et al.* 1985; Helou, Soifer, and Rowan-Robinson 1985; Hummel 1986). We will discuss this second point further in § IV*c*. All the other well-defined correlations of either B or X with any of the variables H, R, and FIR follow power-law functions with exponents $\alpha \sim 0.5$–0.7. This implies that different emission properties do not simply scale with luminosity, and that other factors are relevant. In the attempt to uncover some of these factors, we will examine first the relationships between B, H, and far-infrared luminosities, since these can be related directly to the different components of the stellar population.

The flat correlation between B and H ($l_B \propto l_H^{\sim 0.73}$) was first reported by Aaronson, Huchra, and Mould (1979). It could be caused by relatively higher fraction of early-type stars in galaxies of low luminosity and late morphological type, which would increase their blue luminosity (Aaronson, Huchra, and Mould 1979; Tully, Mould, and Aaronson 1982). In principle, a relative excess of extinction in the more luminous galaxies could also explain the data. Any such explanations should now be checked for consistency against the equally flat relationship between B and FIR, since the far-infrared emission is largely due to reprocessed stellar light with different types of stars contributing different amounts (e.g., Cox, Krügel, and Mezger 1986). As discussed below, neither the extinction scenario nor the presence of starburst activity in the less luminous galaxies is consistent with our results. A luminosity dependence of the initial mass function (IMF) or a bimodal IMF (Larson 1986) is consistent with the data, if coupled with the presence of "warm" starburst components in the far-infrared emission of the more luminous galaxies.

i) *Extinction*

The presence of extinction in the more luminous systems would have the desired effect of depressing the blue light, but not the H and far-infrared emission, thus explaining the observations. Extinction alone, however, is unlikely to account for the observed trend completely, since the amount needed is largely in excess of the expected values. An extinction of ~ 2.5 mag (above average galactic values; de Vaucouleurs, de Vaucouleurs, and Corwin 1976) would be required in the most luminous galaxies. This value is even higher than the high values measured in H II regions ($A_v \sim 1.7$ mag; e.g., Israel and Kennicutt 1980).

An independent estimate of the average excess extinction based on the slope of the correlation between X-ray and optical (B) luminosities supports this conclusion. On the assumption of an intrinsic linear relationship between the two luminosities, and of a relatively hard ($kT \gtrsim 2$ keV) X-ray spectrum (consistent with the average X-ray spectrum of spiral galaxies: Fabbiano and Trinchieri 1987), the deviation at high luminosities between the observed average X-ray to optical flux ratio and the one predicted on the basis of a linear relationship can be used to estimate an average extinction (see Trinchieri, Fabbiano, and Palumbo 1985). Given the results of Table 5 in the Appendix, we find that no more than ~ 1.3 mag of extinction in B is allowed. Since binary X-ray sources, which are likely to contribute a substantial fraction of the X-ray emission (e.g., Fabbiano 1986 and references therein), often present intrinsic absorption, the above estimate is likely to be generous.

ii) *More Recent Star Formation or Flatter IMF in Low-Luminosity Galaxies*

If extinction is not the cause of the flat (B, FIR) and (B, H) correlations, then these relationships must be related to the intrinsic stellar composition. An enhancement of the B emission of the less luminous/massive galaxies due to bursts of recent star formation, however, is not a likely explanation, since in this case one would also expect a parallel increase of the far-infrared emission in these galaxies. The latter could be even larger than the increase in the blue if, as is likely, the newly formed stars appear in dusty regions. This would lead to a steeper relationship between B and FIR than between B and H, contrary to the observations. In this scenario one would also expect the less luminous galaxies to have warmer far-infrared colors than the more luminous ones, also contrary to the observations (e.g., Helou 1986).

The observed relationships could be consistent instead with a steepening of the IMF in more massive/luminous galaxies coupled with an increase of the specific star formation rate with increasing galaxy mass (Tully, Mould, and Aaronson 1982). This would cause a relative excess of H-band emission in these galaxies, without affecting the far-infrared colors. Alternatively, a bimodal IMF in spiral galaxies with the relative amounts of the massive and low-mass components varying with galaxy mass/luminosity (Larson 1986) would be also consistent with our data. In this latter picture, the proportionality between B and X-ray luminosities would suggest that the X-ray sources belong predominantly to the massive stellar component ($M > 1\ M_\odot$). In either case, however, an additional explanation is needed for the relative increase of FIR in the more luminous galaxies. We discuss below how the "warm" far-infrared com-

ponent, which is found prevalently in these galaxies, can explain our results.

iii) *Starburst Activity in High-Luminosity Galaxies*

The presence of a "warm" far-infrared component linked to strong starburst activity in dusty regions (possibly nuclear; Rowan-Robinson and Crawford 1986) might be responsible for the flat relationship between B and FIR, by causing a larger increment in the far-infrared than in the optical emission of more luminous galaxies. We have investigated this with a sample of normal late-type spirals ($T = 4$–10) decomposed into two far-infrared components—cool disk and warm starburst—by Rowan-Robinson and Crawford (1986). The plots of the B luminosity against these two far-infrared components are shown in Figures 8*a* and 8*b*, respectively, and suggest a flatter relationship between the optical (B) luminosity and the starburst component (see also Helou 1986).

If the extinction in the warm FIR emitting regions is very high, as it might be in nuclear starburst regions (e.g., Lebofsky and Rieke 1979; Becklin *et al.* 1980), these would not contribute much to the total B emission, and therefore the previous discussion on the (B, H) correlation would still be valid. It is also possible, depending on their age, that these stellar clusters contain a considerable amount of red supergiants. These could increase the H-band emission of more luminous spirals and contribute to flattening the (B, H) correlation.

Violent widespread starburst activity in galaxies can result in an increase of the X-ray emission, relative to galaxies of similar optical magnitude and redder colors (Fabbiano, Feigelson, and Zamorani 1982; Fabbiano, Trinchieri, and Macdonald 1984). However, the linear (X, B) relationship shows that the X-ray luminosity of the luminous late-type spirals is not affected significantly. This is not necessarily a problem with our previous discussion, since detailed observations of luminous galaxies with normal average colors but with starburst nuclear regions (e.g., NGC 253, NGC 6946, M83; Fabbiano and Trinchieri 1984, 1987; Trinchieri, Fabbiano, and Palumbo 1985) show that the nuclear source, although dominating the far-infrared, contributes to only a fraction of the total X-ray emission.

c) *The Origin of the Nonthermal Radio Continuum Emission of Spiral Galaxies*

As discussed in § I, there is conflicting evidence bearing upon the nature of the nonthermal radio continuum emission of spiral galaxies. In particular, can one exclude sources of cosmic-ray electrons belonging to the old disk population; and is there a direct link between X-ray and cosmic-ray sources, as suggested by FT85?

Looking at our results, we can only exclude with some confidence that the very old stellar component dominating in the H band contributes significantly to the radio emission. Very good correlations are instead observed between the radio and the far-infrared and X-ray luminosities. Of these, the radio–far-infrared correlation is formally the strongest. Moreover, it is the only one with a power-law slope of the order of unity. This proportionality suggests that any conclusion on the galactic component responsible for the radio emission is linked to our understanding of the nature of the far-infrared emission.

The recent idea of a multicomponent FIR emission in spiral galaxies, with a large contribution from the general stellar disk population (Cox, Krügel, and Mezger 1986; Rowan-Robinson and Crawford 1986; Persson and Helou 1987), questions the association of the radio emission solely with recent star formation (e.g., Helou, Soifer, and Rowan-Robinson 1985; de Jong *et al.* 1985) and makes any simple explanation uncertain (Helou 1986). However, the proportional increase of the radio and far-infrared relative to B in the high-luminosity late-type galaxies is reminiscent of what is observed in a more extreme way in starburst galaxies (Klein 1985; Kunth and Sevre 1985). If the warm FIR "starburst" component is responsible for the nonlinearity of the (B, FIR) correlation (§ IV*b*[iii]), this proportionality suggests a link of the radio emission (and cosmic-ray production) with the very young Population I. An older disk origin of the radio emission of the less luminous galaxies is, however, not excluded, since in these galaxies the far-infrared emission is dominated by the cool "disk" component (Fig. 8; Helou 1986; see also FT85). A definitive answer to the question of the nature of the cosmic-ray sources in galaxies will have to be postponed until correlations of the radio emission with the cool and warm components can be studied and many radio and far-infrared maps can be compared in detail.

Our statistical analysis suggests that the correlation between X-ray and radio continuum of late-type spirals is stronger than that between far-infrared and X-ray luminosities (Fig. 5). This result could indicate a direct astrophysical link between X-ray and radio emission, rather than a link through the stellar population responsible for the far-infrared emission. This

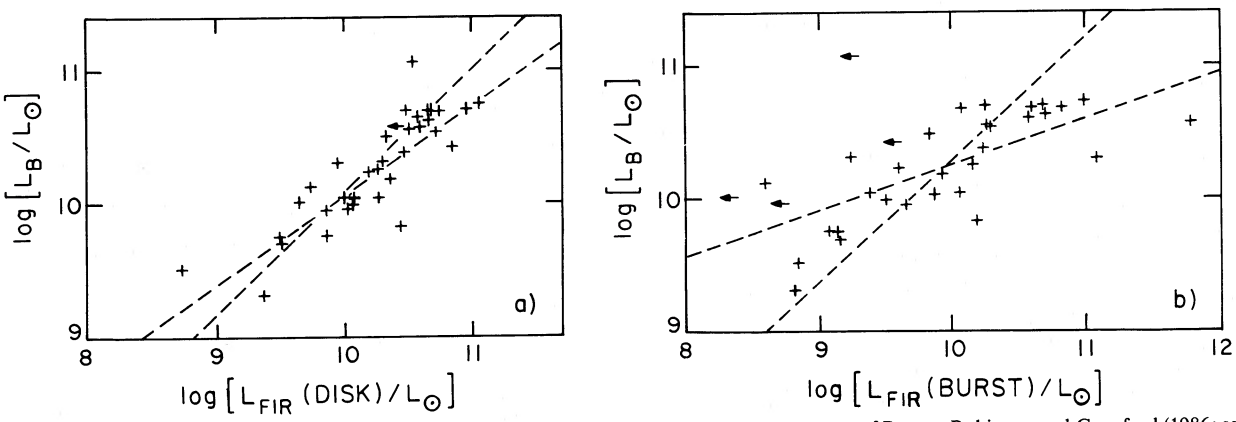

FIG. 8.—Plots of the relationships between optical (B) luminosity L_B and the two far-infrared components of Rowan-Robinson and Crawford (1986; see text). (*a*) L_B vs. L_{FIR}(disk); (*b*) L_B vs. L_{FIR}(burst). All quantities are taken from Rowan-Robinson and Crawford and are in solar units. The dashed lines are our regression lines: (*a*) $\log L_B = (0.68^{+0.12}_{-0.07}) \log L_{FIR}(\text{disk}) + 3.1 \pm 2.0$ and $\log L_{FIR}(\text{disk}) = (1.07^{+0.17}_{-0.15}) \log L_B - 0.7 \pm 1.8$; (*b*) $\log L_B = (0.35^{+0.05}_{-0.08}) \log L_{FIR}(\text{burst}) + 6.9 \pm 0.7$ and $\log L_{FIR}(\text{burst}) = (1.21^{+0.34}_{-0.20}) \log L_B - 3.3 \pm 2.7$.

would be in agreement with the suggestion of FT85 (see also Palumbo *et al.* 1985) that X-ray sources contribute to the production of cosmic rays in spiral galaxies.

In late-type spirals the strong correlation of the X-ray luminosity (and the weaker one of the *B* luminosity) with the radio continuum emission can be represented by a power law with exponent $\alpha \sim 0.6$. On the assumption of proportionality between the sources of cosmic rays and the X-ray emitting population, FT85 suggested that this flat power-law slope could imply a luminosity dependence of the galaxies' magnetic field intensity. Estimates of magnetic field intensity from radio measurements, however, do not show such a trend (Beck and Reich 1985). As discussed above, the strong linear correlation between radio and far-infrared emission suggests that the sources of cosmic-ray electrons are a constant fraction of the stars responsible for heating the dust to far-infrared temperatures. In this case, there is no requirement of a luminosity dependence of the magnetic field intensity. The flat relationship of the radio and X-ray luminosities could instead result from the presence of a compact warm starburst component in high-luminosity galaxies.

V. SUMMARY AND CONCLUSIONS

A statistical analysis of the relationships between global emission properties of spiral galaxies, including the radio continuum, far-infrared, near-infrared *H* band, optical (*B*), and X-ray emission, has led to the following conclusions:

1. Different properties are observed in early-type (Sa–Sb) and in late-type (Sbc and later) spiral galaxies, which can be ascribed to the presence of prominent bulges in the early-type spirals. These would contribute substantially to the emission in the near-infrared (*H*), optical (*B*), and X-ray bands, but not to the radio and possibly not to the far-infrared emission.

2. In late-type spiral galaxies the statistical properties of the emission at different wavelengths are consistent with a common disk/arm origin. With the exclusion of the near-infrared *H*-band emission, which is dominated by the old stellar population (Aaronson, Huchra, and Mould 1979), the luminosities at all the other wavelengths (FIR, R, *B*, X) are well correlated with one another. The emission in the optical (*B*) is also well correlated with *H*, indicating that older and younger stars both contribute to it.

3. The power-law exponents of the correlations are consistent with a steeper IMF in low-luminosity galaxies and with the presence of an obscured starburst component in high-luminosity galaxies.

4. The strongest correlation of the radio continuum luminosity with any other variable is with the far-infrared, suggesting that the radio emission is disjoint from the older low-mass stellar component (see also Helou, Soifer, and Rowan-Robinson 1985; de Jong *et al.* 1985; Gavazzi, Cocito, and Vettolani 1986). Since the far-infrared emission of high-luminosity galaxies is likely to be dominated by a warm "starburst" component, we suggest that in these galaxies the cosmic-ray production is linked to the younger stellar population. However, the presence of a different class of cosmic-ray sources dominating the radio emission of low-luminosity galaxies cannot be excluded with the present data. The correlation between X-ray and radio continuum luminosities is also one of the most significant and could suggest a direct link between X-ray and cosmic-ray sources (see FT85). In view of our new results, the suggestion of a luminosity dependence of the magnetic field intensity of spiral galaxies (FT85) is probably no longer viable, but must be replaced with another luminosity dependence such as that of the "warm" starburst component.

We believe that this paper illustrates the necessity of a multifrequency approach to the study of global galaxy properties. It also illustrates the need for a well-selected, unbiased, large sample of galaxies that could be agreed upon by the astronomical community and then observed extensively at different wavelengths, to ensure complete coverage from the radio to the X-ray region. Such a study is essential to confirm some of our results and to gain a more general understanding of the structure and evolution of spiral galaxies.

We thank A. Campbell, U. Klein, J. Mathis, C. Persson, N. Panagia, S. Willner, and G. Zamorani for useful discussions; S. Gibbs for assistance in the data analysis; and M. Elvis and B. Wilkes for critical readings of the manuscript. G. T. thanks the Italian Piano Spaziale Nazionale for partial financial support. This work was supported under National Aeronautics and Space Administration contract NAS8-30751.

APPENDIX

We analyzed the VLA and X-ray samples described in § II and a sample obtained by joining them (the "joint" sample) using both nonparametric and parametric tests. Since there are six galaxies in common in the VLA and X-ray samples, the VLA entries for these galaxies were used in the joint sample. Also, the four galaxies with $T = 4$ were excluded from the analysis of this sample, to increase the separation between early- and late-type spirals. Our aim was to establish (1) the statistical significance of correlations between any two variables; (2) their relative strength, i.e., given a group of three or four variables, which correlations are likely to be primary ones and which are likely to be the consequence of these; and (3) the functional relationships between variables. We used the nonparametric Spearman rank test and the multivariate Spearman partial rank test (Kendall and Stuart 1976), and the parametric maximum-likelihood method developed by Avni *et al.* (1980) and extended by Schmitt (1985), to include all detections and bounds (in both axes) in the analysis. Previous applications of these techniques and a more detailed explanation can be found in Fabbiano, Feigelson, and Zamorani (1982), FT85, and Fabbiano *et al.* (1987). Unlike the procedure followed in our previous analysis of spiral galaxies (FT85), we calculated regressions on *both* variables for a given pair. This is made possible by the use of Schmitt's (1985) approach. This method gives a better definition of the power-law slope of the correlations, since the slope of the "true" underlying relationships is likely to be in between the two measured regressions. The results of this analysis are given in Tables 3–9.

We checked for beam-size effects in the radio flux densities (see § II*a*) by repeating the analysis using the 20 cm flux densities of Hummel (1980) for the galaxies whose fluxes are likely to be underestimated in the Gioia and Fabbiano (1987) survey. The results are not significantly different. They are given in parentheses in Tables 3 and 7 for the nonparametric tests. No appreciable differences were found in the parametric analysis.

TABLE 3

SPEARMAN RANK PROBABILITIES (one-tailed) FOR CORRELATIONS[a,b]

	VLA SAMPLE				JOINT SAMPLE			
	T = 1–3		T = 6–9		T = 0–3		T = 5–10	
CORRELATIONS	N	P	N	P	N	P	N	P
l_R, l_B	25	8×10^{-3}	20	5×10^{-7} ($<5 \times 10^{-7}$)	37	5×10^{-5}	35	$\ll 5 \times 10^{-7}$ ($\ll 5 \times 10^{-7}$)
l_R, L_{FIR}	22	$\ll 5 \times 10^{-7}$	19	$\ll 5 \times 10^{-7}$ ($<5 \times 10^{-7}$)	34	$\ll 5 \times 10^{-7}$	31	$\ll 5 \times 10^{-7}$ ($\ll 5 \times 10^{-7}$)
L_{FIR}, l_B	22	3×10^{-3}[c]	19	5×10^{-7}	41	1×10^{-5}	36	$\ll 5 \times 10^{-7}$

[a] The numbers in parenthesis are obtained when Hummel's 1980 radio continuum fluxes are used (see text).
[b] N is the number of objects and P is the probability of a chance correlation.
[c] If the limits in L_{FIR} are included, one obtains $P \geq 5\%$ for $N = 25$.

TABLE 4

SPEARMAN RANK PROBABILITIES (one-tailed) FOR CORRELATION: X-RAY SAMPLE[a]

	T = 0–3		T = 4–10		TOTAL	
CORRELATIONS	N	P	N	P	N	P
l_R, l_H	12	7×10^{-3}	15	$\sim 5 \times 10^{-4}$	27	5×10^{-5}
l_R, l_B	14	5×10^{-3}	22	5×10^{-6}	36	$<5 \times 10^{-7}$
l_R, l_x	13	1×10^{-4}	20	$\ll 5 \times 10^{-7}$	33	$\ll 5 \times 10^{-7}$
l_R, L_{FIR}	14	5×10^{-5}	19	$\ll 5 \times 10^{-7}$	33	$\ll 5 \times 10^{-7}$
l_H, l_B	16	$\ll 5 \times 10^{-7}$	19	$\ll 5 \times 10^{-7}$	35	$\ll 5 \times 10^{-7}$
l_H, l_x	14	$\sim 5 \times 10^{-4}$	16	1×10^{-5}	30	$<5 \times 10^{-7}$
l_H, L_{FIR}	16	2.5×10^{-3}	15	5×10^{-6}	31	$\sim 5 \times 10^{-6}$
l_B, l_x	17	$<5 \times 10^{-7}$	25	$\ll 5 \times 10^{-7}$	42	$\ll <5 \times 10^{-7}$
l_B, L_{FIR}	21	5×10^{-4}	24	$<5 \times 10^{-7}$	45	$<5 \times 10^{-7}$
l_x, L_{FIR}	17	2.5×10^{-3}	20	$<5 \times 10^{-7}$	37	$<5 \times 10^{-7}$

[a] N is the number of objects and P is the probability of a chance correlation.

TABLE 5

MAXIMUM-LIKELIHOOD CORRELATION COEFFICIENTS AND REGRESSION PARAMETERS: X-RAY SAMPLE

		EARLY (T = 0–3)			LATE (T = 4–10)			TOTAL (T = 0–10)		
Y[a]	X[a]	r_c	A	B	r_c	A	B	r_c	A	B
$\log l_R$	$\log l_H$	$0.75^{+0.08}_{-0.12}$	0.78 ± 0.17	$5.2^{+5.3}_{-4.6}$	0.89 ± 0.04	1.07 ± 0.14	$-2.7^{+4.1}_{-3.6}$	0.82 ± 0.05	0.82 ± 0.10	$4.3^{+2.5}_{-3.2}$
$\log l_H$	$\log l_R$		0.71 ± 0.24	$9.2^{+7.3}_{-6.2}$		0.75 ± 0.10	7.7 ± 3.0		0.81 ± 0.08	5.9 ± 2.2
$\log l_R$	$\log l_B$	$0.83^{+0.07}_{-0.11}$	1.09 ± 0.17	$-3.5^{+5.1}_{-4.4}$	0.85 ± 0.05	$1.31^{+0.18}_{-0.12}$	$-9.6^{+3.8}_{-4.9}$	0.82 ± 0.04	1.14 ± 0.14	$-4.7^{+3.6}_{-4.3}$
$\log l_B$	$\log l_R$		$0.61^{+0.14}_{-0.11}$	$11.6^{+3.3}_{-3.9}$		0.55 ± 0.08	13.0 ± 2.0		0.58 ± 0.06	12.4 ± 1.7
$\log l_R$	$\log l_x$	$0.87^{+0.06}_{-0.09}$	0.92 ± 0.13	8.0 ± 3.0	0.88 ± 0.05	1.28 ± 0.21	$0.2^{+4.4}_{-5.4}$	0.85 ± 0.05	$1.01^{+0.13}_{-0.09}$	$6.0^{+2.0}_{-3.0}$
$\log l_x$	$\log l_R$		0.84 ± 0.15	$-1.8^{+4.9}_{-3.4}$		$0.60^{+0.13}_{-0.09}$	$4.8^{+2.5}_{-3.4}$		0.69 ± 0.09	2.2 ± 2.5
$\log l_R$	$\log L_{FIR}$	$0.89^{+0.04}_{-0.11}$	$1.04^{+0.10}_{-0.23}$	$-16.5^{+9.9}_{-4.8}$	0.95 ± 0.02	$1.01^{+0.05}_{-0.07}$	$-15.1^{+3.0}_{-2.1}$	$0.92^{+0.02}_{-0.04}$	0.94 ± 0.07	-12.1 ± 2.8
$\log L_{FIR}$	$\log l_R$		0.75 ± 0.12	21.8 ± 3.5		$0.89^{+0.05}_{-0.04}$	17.5 ± 1.3		$0.90^{+0.05}_{-0.07}$	17.4 ± 2.0
$\log l_H$	$\log l_B$	0.95 ± 0.03	$1.30^{+0.15}_{-0.23}$	$-8.2^{+3.6}_{-4.3}$	0.96 ± 0.02	$1.31^{+0.10}_{-0.12}$	$-9.0^{+3.6}_{-2.8}$	0.96 ± 0.02	1.41 ± 0.08	$-11.6^{+2.4}_{-2.0}$
$\log l_B$	$\log l_H$		$0.70^{+0.18}_{-0.13}$	$8.5^{+3.7}_{-5.5}$		$0.70^{+0.06}_{-0.04}$	$8.6^{+1.0}_{-2.0}$		0.65 ± 0.03	9.9 ± 1.0
$\log l_H$	$\log l_x$	$0.91^{+0.04}_{-0.10}$	$0.89^{+0.13}_{-0.16}$	$9.9^{+3.6}_{-3.1}$	0.93 ± 0.03	1.24 ± 0.17	$1.6^{+3.7}_{-3.3}$	0.91 ± 0.02	$1.16^{+0.12}_{-0.10}$	$3.7^{+2.1}_{-2.7}$
$\log l_x$	$\log l_H$		$0.93^{+0.08}_{-0.13}$	$-5.2^{+3.8}_{-2.4}$		$0.70^{+0.07}_{-0.05}$	$1.6^{+1.5}_{-1.9}$		0.72 ± 0.05	1.0 ± 1.5
$\log l_H$	$\log L_{FIR}$	$0.45^{+0.17}_{-0.22}$	$0.44^{+0.46}_{-0.24}$	$10.4^{+9.6}_{-20.4}$	0.88 ± 0.04	$0.76^{+0.09}_{-0.12}$	$-3.7^{+5.2}_{-3.9}$	0.77 ± 0.06	$0.79^{+0.13}_{-0.08}$	$-4.7^{+3.3}_{-5.7}$
$\log L_{FIR}$	$\log l_H$		$0.41^{+0.22}_{-0.20}$	$30.9^{+5.6}_{-6.6}$		$1.01^{+0.14}_{-0.10}$	$13.4^{+3.2}_{-3.8}$		0.75 ± 0.11	$20.8^{+3.3}_{-2.7}$
$\log l_B$	$\log l_x$	$0.92^{+0.03}_{-0.05}$	$0.75^{+0.11}_{-0.07}$	$12.3^{+1.7}_{-2.6}$	0.92 ± 0.03	0.83 ± 0.08	$10.5^{+1.7}_{-1.5}$	0.93 ± 0.02	0.81 ± 0.05	11.1 ± 1.0
$\log l_x$	$\log l_B$		$1.11^{+0.12}_{-0.21}$	$-10.1^{+5.4}_{-3.9}$		$1.02^{+0.10}_{-0.07}$	$-7.6^{+2.2}_{-2.7}$		1.07 ± 0.08	$-8.9^{+2.0}_{-2.3}$
$\log l_B$	$\log L_{FIR}$	$0.64^{+0.10}_{-0.13}$	$0.59^{+0.11}_{-0.15}$	$3.6^{+3.3}_{-2.3}$	0.87 ± 0.05	$0.60^{+0.04}_{-0.05}$	3.1 ± 2.0	$0.79^{+0.04}_{-0.06}$	0.60 ± 0.05	$3.0^{+4.7}_{-2.4}$
$\log L_{FIR}$	$\log l_B$		0.73 ± 0.18	$21.8^{+6.5}_{-5.1}$		$1.27^{+0.20}_{-0.22}$	$6.2^{+6.3}_{-5.5}$		$1.04^{+0.10}_{-0.13}$	$12.7^{+4.0}_{-2.8}$
$\log l_x$	$\log L_{FIR}$	0.65 ± 0.13	$0.68^{+0.34}_{-0.21}$	$-7.3^{+9.2}_{-14.6}$	0.87 ± 0.05	0.60 ± 0.07	$-3.9^{+3.2}_{-3.0}$	$0.81^{+0.04}_{-0.06}$	$0.65^{+0.05}_{-0.07}$	$-6.2^{+3.1}_{-2.1}$
$\log L_{FIR}$	$\log l_x$		$0.59^{+0.19}_{-0.17}$	$29.9^{+3.8}_{-4.1}$		$1.28^{+0.11}_{-0.17}$	$14.7^{+3.8}_{-2.5}$		$0.98^{+0.16}_{-0.12}$	$21.3^{+2.7}_{-3.5}$

[a] $Y = AX + B$; r_c is the correlation coefficient. The uncertainties on r_c, A, and B are at the 68% confidence level.

TABLE 6

MAXIMUM-LIKELIHOOD CORRELATION COEFFICIENTS AND REGRESSION PARAMETERS: JOINT SAMPLE

		EARLY (T = 0–3)			LATE (T = 5–10)		
Y[a]	X[a]	r_c	A	B	r_c	A	B
$\log l_R$	$\log l_B$	$0.67^{+0.08}_{-0.10}$	0.99 ± 0.16	$-0.6^{+4.9}_{-4.7}$	$0.85^{+0.03}_{-0.05}$	$1.66^{+0.14}_{-0.22}$	$-19.6^{+6.3}_{-4.2}$
$\log l_B$	$\log l_R$		0.45 ± 0.10	$16.3^{+3.2}_{-2.7}$		$0.44^{+0.04}_{-0.03}$	$16.3^{+0.9}_{-1.0}$
$\log l_R$	$\log L_{FIR}$	$0.87^{+0.03}_{-0.04}$	1.06 ± 0.11	$-17.6^{+4.9}_{-4.7}$	$0.91^{+0.04}_{-0.03}$	$0.93^{+0.12}_{-0.08}$	$-11.7^{+3.4}_{-5.2}$
$\log L_{FIR}$	$\log l_R$		$0.72^{+0.06}_{-0.07}$	$22.9^{+1.8}_{-1.6}$		0.89 ± 0.07	17.8 ± 2.2
$\log L_{FIR}$	$\log l_B$	$0.58^{+0.08}_{-0.10}$	$0.68^{+0.11}_{-0.15}$	$23.3^{+4.4}_{-3.2}$	0.88 ± 0.03	$1.49^{+0.17}_{-0.16}$	$0.0^{+3.5}_{-5.4}$
$\log l_B$	$\log L_{FIR}$		$0.50^{+0.09}_{-0.10}$	$7.1^{+4.7}_{-3.1}$		$0.52^{+0.05}_{-0.04}$	$6.5^{+1.7}_{-2.3}$

[a] $Y = AX + B$; r_c is the correlation coefficient. The uncertainties on r_c, A, and B are at the 68% confidence level.

TABLE 7

SPEARMAN PARTIAL RANK PROBABILITIES (one-tailed) FOR CORRELATIONS BETWEEN l_R, l_B, L_{FIR}: VLA AND JOINT SAMPLES[a,b]

	VLA SAMPLE				JOINT SAMPLE			
	T = 1–3		T = 6–9		T = 0–3		T = 5–10	
CORRELATIONS $X, Y.Z$[c]	N	P	N	P	N	P	N	P
R, B. FIR	22	>40%	19	15% (3%)	34	2%	31	13% (8%)
R, FIR. B	22	$<5 \times 10^{-7}$	19	0.5% (1%)	34	$<5 \times 10^{-7}$	31	1×10^{-5} (1×10^{-5})
FIR, B. R	22	15%	19	4% (5%)	34	>40%	31	0.2% (0.7%)

[a] The numbers in parenthesis are obtained when Hummel's 1980 radio continuum fluxes are used (see text).
[b] N is the number of objects in each subsample used for the test, and P is the probability of chance correlation.
[c] X and Y are the two variables being tested for correlation, under the hypothesis that the variable Z does not vary.

TABLE 8

SPEARMAN PARTIAL RANK PROBABILITIES (one-tailed): THREE-VARIABLE TESTS (l_R, l_H, l_B, l_x, L_{FIR})

	T = 0–3		T = 4–10		TOTAL			T = 0–3		T = 4–10		TOTAL	
CORRELATIONS $X, Y.Z$[a]	N	P[b]	N	P[b]	N	P[b]	CORRELATIONS X, Y, Z[a]	N	P[b]	N	P[b]	N	P[b]
R, H. B	12	29%	15	12%	27	>40%	R, X. FIR	13	7×10^{-4}	17	0.8%	30	5×10^{-5}
R, B. H	12	12%	15	16%	27	0.6%	R, FIR. X	13	1×10^{-5}	17	5×10^{-5}	30	1×10^{-7}
H, B. R	12	1×10^{-6}	15	0.5%	27	5×10^{-7}	X, FIR. R	13	5%[c]	17	35%	30	25%
R, H. X	11	33%	13	20%	24	33%	H, B. X	14	1×10^{-4}	16	5%	30	0.1%
R, X. H	11	4%	13	0.3%	24	5×10^{-5}	H, X. B	14	26%	16	38%	30	26%
H, X. R	11	4%	13	18%	24	5×10^{-4}	B, X. H	14	1%	16	1×10^{-4}	30	5×10^{-6}
R, H. FIR	12	8%	12	20%	24	8%	H, B. FIR	16	0.1%	15	0.2%	31	$<5 \times 10^{-7}$
R, FIR. H	12	0.7%	12	0.2%	24	5×10^{-6}	H, FIR. B	16	34%	15	2%	31	30%
H, FIR. R	12	>40%	12	25%	24	28%	B, FIR. H	16	7%	15	>40%	31	2%
R, B. X	13	35%	20	36%	33	31%	H, X. FIR	14	0.7%	12	19%	26	1×10^{-4}
R, X. B	13	1%	20	5×10^{-4}	33	5×10^{-4}	H, FIR. X	14	9%	12	7%	26	19%
B, X. R	13	0.2%	20	0.7%	33	5×10^{-6}	X, FIR. H	14	28%	12	3%	26	2%
R, B. FIR	14	3%	19	6%	33	0.7%	B, X. FIR	17	1×10^{-5}	20	0.5%	37	$<5 \times 10^{-7}$
R, FIR. B	14	5×10^{-4}	19	$<5 \times 10^{-7}$	33	$<5 \times 10^{-7}$	B, FIR. X	17	25%	20	35%	37	24%
B, FIR. R	14	27%	19	>40%	33	35%	X, FIR. B	17	24%	20	0.5%	37	2%

[a] X and Y are the two variables being tested for correlation, under the hypothesis that the variable Z does not vary.
[b] N is the number of objects in each subsample, and P is the probability of chance correlation.
[c] Anticorrelation.

TABLE 9

SPEARMAN PARTIAL RANK PROBABILITIES (one-tailed): FOUR-VARIABLE TESTS (l_R, l_H, l_B, l_x, L_{FIR})

CORRELATIONS $X, Y. Z, W$[a]	$T = 0$–3		$T = 4$–10		TOTAL	
	N	P[b]	N	P[b]	N	P[b]
R, *H*. *B*, X	11	40%	13	7%	24	23%
R, *B*. *H*, X	11	>40%	13	9%	24	24%
R, X. *H*, *B*	11	12%	13	0.6%	24	0.5%
H, *B*. R, X	11	1×10^{-4}	13	0.9%	24	0.3%
H, X. R, *B*	11	10%	13	9%	24	24%
B, X. R, *H*	11	2%	13	0.1%	24	0.9%
R, *H*. *B*, FIR	12	35%	12	>40%	24	17%
R, *B*. *H*, FIR	12	23%	12	16%	24	1%
R, FIR. *H*, *B*	12	2%	12	0.1%	24	5×10^{-6}
H, *B*. R, FIR	12	5×10^{-6}	12	2%	24	1×10^{-6}
H, FIR. R, *B*	12	>40%	12	17%	24	12%
B, FIR. R, *H*	12	>40%	12	21%	24	15%
R, *B*. X, FIR	13	33%	17	21%	30	>40%
R, X. *B*, FIR	13	1.6%	17	8%	30	0.5%
R, FIR. *B*, X	13	5×10^{-4}	17	5×10^{-5}	30	5×10^{-6}
B, X. R, FIR	13	0.6%	17	3%	30	2×10^{-5}
B, FIR. R, X	13	39%	17	26%	30	34%
X, FIR. R, *B*	13	11%	17	>40%	30	22%
H, *B*. X, FIR	14	7×10^{-4}	12	0.7%	26	0.2%
H, X. *B*, FIR	14	27%	12	5%[c]	26	>40%
H, FIR. *B*, X	14	>40%	12	1%	26	22%
B, X. *H*, FIR	14	1.7%	12	1×10^{-4}	26	5×10^{-5}
B, FIR. *H*, X	14	20%	12	2%[c]	26	>40%
X, FIR. *H*, *B*	14	>40%	12	0.5%	26	6%
R, *H*. X, FIR	11	>40%	10	28%	21	14%
R, X. *H*, FIR	11	2%	10	9%	21	3×10^{-4}
R, FIR. *H*, X	11	1%	10	6%	21	1×10^{-5}
H, X. R, FIR	11	4%	10	40%	21	0.2%
H, FIR. R, X	11	25%	10	34%	21	15%
X, FIR. R, *H*	11	12%	10	>40%	21	9%

[a] X and Y are the two variables being tested for correlation, under the hypothesis that Z and W do not vary.

[b] N is the number of objects in each subsample, and P is the probability of a chance correlation.

[c] Anticorrelation.

REFERENCES

Aaronson, M., Huchra, J., and Mould, J. 1979, *Ap. J.*, **229**, 1.
Avni, Y., Soltan, A., Tananbaum, H., and Zamorani, G. 1980, *Ap. J.*, **238**, 800.
Beck, R., and Reich, W. 1985, in *IAU Symposium 106, The Milky Way Galaxy*, ed. H. van Woerden, R. J. Allen, and W. Butler-Burton (Dordrecht: Reidel), p. 239.
Becklin, E. E., Gatley, I., Matthews, K., Neugebauer, G., Sellgren, K., Werner, M. W., and Wynn-Williams, C. G. 1980, *Ap. J.*, **236**, 441.
Catalogued Galaxies and Quasars Observed in the IRAS Survey. 1985, prepared by C. J. Lonsdale, G. Helou, J. C. Good, and W. Rice (Pasadena: JPL).
Cox, P., Krügel, E., and Mezger, P. G. 1986, *Astr. Ap.*, **155**, 380.
de Jong, T. 1986, in *Spectral Evolution of Galaxies*, ed. C. Chiosi and A. Renzini (Dordrecht: Reidel), p. 111.
de Jong, T., Klein, U., Wielebinski, R., and Wunderlich, E. 1985, *Astr. Ap.*, **147**, L6.
de Vaucouleurs, G., de Vaucouleurs, A., and Corwin, H. G. 1976, *Second Reference Catalogue of Bright Galaxies* (Austin: University of Texas Press).
Fabbiano, G. 1986, *Pub. A.S.P.* **98**, 525.
Fabbiano, G., Feigelson, E., and Zamorani, G. 1982, *Ap. J.*, **256**, 397.
Fabbiano, G., Klein, U., Trinchieri, G., and Wielebinski, R. 1987, *Ap. J.*, **312**, 111.
Fabbiano, G., and Trinchieri, G. 1984, *Ap. J.*, **286**, 491.
———. 1985, *Ap. J.*, **296**, 430 (FT85).
———. 1987, *Ap. J.*, **315**, 46.
Fabbiano, G., Trinchieri, G., and Macdonald, A. 1984, *Ap. J.*, **284**, 65.
Feigelson, E. D., and Berg, C. J. 1983, *Ap. J.*, **269**, 400.
Gavazzi, G., Cocito, A., and Vettolani, G. 1986, *Ap. J.* (*Letters*), **305**, L15.
Gioia, I. M., and Fabbiano, G. 1987, *Ap. J. Suppl.*, **63**, 771.
Gioia, I. M., and Gregorini, L. 1980, *Astr. Ap. Suppl.*, **41**, 329.
Helou, G. 1986, *Ap. J.* (*Letters*), **311**, L33.
Helou, G., Soifer, B. T., and Rowan-Robinson, M. 1985, *Ap. J.* (*Letters*), **298**, L7.
Hummel, E. 1980, *Astr. Ap. Suppl.*, **41**, 151.
———. 1981, *Astr. Ap.*, **93**, 93.
———. 1986, *Astr. Ap.*, **160**, L4.
Israel, F. P., and Kennicutt, R. C. 1980, *Ap. Letters*, **21**, 1.
Kendall, M., and Stuart, A. 1976, *Advanced Theory of Statistics*, Vol. **2** (3d ed.; London: Charles Griffin & Co.).
Kennicutt, R. 1983, *Astr. Ap.*, **120**, 219.
Kent, S. M. 1985, *Ap. J. Suppl.*, **59**, 115.
Klein, U. 1982, *Astr. Ap.*, **116**, 175.
———. 1985, in *Star-forming Dwarf Galaxies and Related Objects*, ed. D. Kunth, T. X. Thuan, and J. T. T. Van (Gif-sur-Yvette: Editions Frontières), p. 371.
Kunth, D., and Sevre, F. 1985, in *Star-forming Dwarf Galaxies and Related Objects*, ed. D. Kunth, T. X. Thuan, and J. T. T. Van (Gif-sur-Yvette: Editions Frontières), p. 331.
Larson, R. B. 1986, *M.N.R.A.S.*, **218**, 409.
Lebofsky, M. J., and Rieke, G. H. 1979, *Ap. J.*, **229**, 111.
Lequeux, J. 1971, *Astr. Ap.*, **15**, 42.
Long, K. S., and Van Speybroeck, L. P. 1983, in *Accretion Driven X-Ray Sources*, ed. W. Lewin and E. P. J. van den Heuvel (Cambridge: Cambridge University Press), p. 41.
Palumbo, G. G. C., Fabbiano, G., Fransson, C., and Trinchieri, G. 1985, *Ap. J.*, **298**, 259.
Persson, C. J., and Helou, G. 1987, *Ap. J.*, **314**, 513.
Rice, W., *et al.* 1987, in preparation.

Rowan-Robinson, M., and Crawford, J. 1986, preprint.
Sandage, A. and Tammann, G. A. 1981, *A Revised Shapley-Ames Catalog of Bright Galaxies* (Publication 635; Washington, DC: Carnegie Institution of Washington).
Schmitt, J. H. M. M. 1985, *Ap. J.*, **293**, 178.
Simien, F., and de Vaucouleurs, G. 1983, in *IAU Symposium 100, Internal Kinematic and Dynamics of Galaxies*, ed. E. Athanassoula (Dordrecht: Reidel), p. 375.
Trinchieri, G., Fabbiano, G., and Palumbo, G. G. C. 1985, *Ap. J.*, **290**, 96.
Tully, R. B., Mould, J. R., and Aaronson, M. 1982, *Ap. J.*, **257**, 527.
van der Kruit, P. C., Allen, R. J., and Rots, A. H. 1977, *Astr. Ap.*, **55**, 421.
Whitmore, B. C. 1984, *Ap. J.*, **278**, 61.

G. FABBIANO and I. M. GIOIA: High Energy Astrophysics Division, Center for Astrophysics, 60 Garden Street, Cambridge, MA 02138

G. TRINCHIERI: Osservatorio Astrofisico di Arcetri, Largo E. Fermi 5, 50125 Firenze, Italy